symmetry

MDPI

*Review*

# Symmetry and Aesthetics in Dentistry

**Christoph Runte and Dieter Dirksen ***

Department of Prosthodontics and Biomaterials, University of Münster, Albert-Schweitzer-Campus 1, 48149 Münster, Germany; crunte@uni-muenster.de
* Correspondence: dirksdi@uni-muenster.de

**Abstract:** Animal bodies in general and faces in particular show mirror symmetry with respect to the median-sagittal plane, with exceptions rarely occurring. Bilateral symmetry to the median sagittal plane of the body also evolved very early. From an evolutionary point of view, it should therefore have fundamental advantages, e.g., more effective locomotion and chewing abilities. On the other hand, the recognition of bilaterally symmetric patterns is an important module in our visual perception. In particular, the recognition of faces with different spatial orientations and their identification is strongly related to the recognition of bilateral symmetry. Maxillofacial surgery and Dentistry affect effective masticatory function and perceived symmetry of the lower third of the face. Both disciplines have the ability to eliminate or mitigate asymmetries with respect to form and function. In our review, we will demonstrate symmetric structures from single teeth to the whole face. We will further describe different approaches to quantify cranial, facial and dental asymmetries by using either landmarks or 3D surface models. Severe facial asymmetries are usually caused by malformations such as hemifacial hyperplasia, injury or other diseases such as Noma or head and neck cancer. This could be an important sociobiological reason for a correlation between asymmetry and perceived disfigurement. The aim of our review is to show how facial symmetry and attractiveness are related and in what way dental and facial structures and the symmetry of their shape and color influence aesthetic perception. We will further demonstrate how modern technology can be used to improve symmetry in facial prostheses and maxillofacial surgery.

**Keywords:** facial symmetry; Asymmetry Index; attractiveness; aesthetic perception; disfigurement



**Citation:** Runte, C.; Dirksen, D. Symmetry and Aesthetics in Dentistry. *Symmetry* **2021**, *13*, 1741. https://doi.org/10.3390/sym13091741

Academic Editors: Carlos Miguel Marto, Mafalda Laranjo, Ana Cristina Gonçalves and Sergei D. Odintsov

Received: 19 July 2021
Accepted: 9 September 2021
Published: 19 September 2021



## 1. Introduction

A large proportion of Eumetazoa shows a bilaterally symmetric body plan. Though adult echinoderms develop pentameral symmetry, they are bilaterally symmetric at least at their larval stage [1]. Exceptions, especially with regard to the head and face, are rare. Recent studies indicate that cranial asymmetry in flatfish seems to have evolved within a short time (approximately 3 million years) as an adaptation to lying on one-half of their body on the seabed [2]. Therefore, bilateral symmetry of the body obviously is an advantageous property in general.

Bilateral symmetry can be seen as a necessary prerequisite for well-proportionedness, since bilaterally symmetrical structures have equal dimensions (1:1 proportion). Asymmetrical faces, therefore, are also disproportioned by definition. On the other hand, bilateral symmetry is not a sufficient condition for well-proportionedness, since the property of bilateral symmetry does not impose any conditions on proportions in the direction of the plane of symmetry. In early mammals, the evolution of molars, premolars, canines, and incisors from haplodont origins has taken place mirror-symmetrical on both sides and equally in the maxilla and mandible. In humans, two incisors, one canine, two premolars and three molars are equally positioned on both sides of the upper as well as of the lower jaw. Eruption time of deciduous and permanent teeth exhibits bilateral symmetry with only minor deviations. However, there is no exact mirror symmetry to the horizontal occlusal plane with regard to maxillary and mandibular teeth in terms of size, shape, angulation

and eruption time [3–5]. A single tooth exhibits only limited mirror symmetry along a mesiodistal or oral–vestibular axis.

In dentistry, bilateral symmetry is usually presumed as beneficial. The self-evidence with which bilateral symmetry is taken for granted can be well judged by the fact that articulators are usually bilaterally symmetrically constructed and mean values of condylar movement are set symmetrically, unless individual data are available [6].

However, especially during the last two decades, new technologies have been introduced and enhanced 3D treatment planning and implementation. This includes facial, intraoral and cast scanning technologies, cone beam-computed tomography and digital technology capable of 3D data processing with respect to bilateral symmetry. Titanium mini-implants have improved the possibility to focus orthodontic treatment on one side of the upper dental arch; individually custom-made implants can be planned and fabricated to augment or replace missing or underdeveloped bony structures; distraction osteogenesis enables treatment to be performed until a symmetric condition is achieved; and prosthodontic appliances can be designed by mirroring the healthy to the affected side.

## 2. Symmetry Perception and Aesthetic Judgement

Recognizing symmetry is a process dependent on neurophysiological fundamentals of visual perception. After entering the eye bulb, light is transformed into neuronal signals in several steps within the retina. The signal from a defined retinal area corresponds to the location of the light source. With stereoscopy, we are able to perceive visible objects spatially over a certain range of distances. From this visual information, outlines with strong light–dark contrast are extracted for object perception and identification purposes. The underlying process, which was elucidated in particular by the experiments of Hubel and Wiesel [7,8], is primarily located in the corpus geniculatum laterale [9] and is considered to be an essential part of pattern recognition, including symmetry perception. The recognition of outlines with brightness contrast starts a process of "tracking" structures with eye movements, by which pattern identification is continued and expanded [10]. When looking at human faces, this draws attention to the corner points of the so called "Yarbus triangle", the eyes and the mouth [11].

It was found that less information increases the rated attractiveness [12]. If the observed face is blurred by low-pass filtering, this mainly affects the outlines necessary for pattern recognition. Face recognition is hindered and delayed by this [13]. The same is true for hemifacial occlusion of the face [12]. It has been shown that in humans and other animals, the ability to complete missing information by using mental images has evolved [14]. This capability enables us to look for necessary information in the right place and to perceive the actual situation more quickly, but it also leads us to complete occluded hemifaces perfectly symmetrically and to perceive blurred faces without disfiguring details.

As a special feature in face recognition, attention is directed mainly to the observed faces' right hemiface, irrespective of special facial properties [15]. This corresponds to an asymmetry of observer brain activity distribution during facial recognition [16] and the beholders also seem to rate attractiveness and some character traits with an emphasis on one half of the observed subjects' face. Although this is not the case for all traits examined, in terms of attractiveness, this applies also to the right hemiface [17,18].

Bilateral facial asymmetry is perceived by laypersons if it exceeds a difference of 3 mm at the oral commissure line edges or the brows, or both [19] and most observers correctly detected asymmetry at a difference of 2 mm or more in eyelid closure [20]. Zamanian et al. found an inconsistency between asymmetry detection between laypersons and dental professionals, but it was not statistically significant [21]. Whether frequent visual examination of faces or professional education with respect to symmetry by dentists, orthodontists or maxillofacial surgeons could improve facial asymmetry perception skills cannot be conclusively assessed based on current research. Some authors found significant differences in facial asymmetry detection skills [22], while others could not confirm a significant difference between laypersons and professionals [18,23]. Perception of asymmetry also

has a temporal dimension; i.e., asymmetric movements, especially when the blink reflex is delayed on one side, affect asymmetry perception and judgement [24].

When facial asymmetry becomes disfiguring, psychosocial consequences have to be taken into consideration [25–27]. Faces above a critical degree of disfigurement, including asymmetry, will cause disgust in the eye of the observer, as has been shown by Shanmugarajah et al. [28] with the possible consequence of comparatively limited opportunities in life for the affected person [29]. According to Higgins [30], disfigurement leads to a discrepancy between the actual and the ideal self, and depression might be the consequence.

## 3. Asymmetry Quantification

Asymmetry quantification has been a topic of anthropometric studies of the human face for a long time. The bust of Nefertiti exhibits a high degree of symmetry and although we do not know anything about the sculptor, it is obvious that symmetry was intuitively assumed as the norm in a healthy human face. In his four books on human proportion, Albrecht Duerer used exactly symmetrical schemes for his depicted faces based on the data of his own anthropometric studies [31]. However, with more sophisticated measuring methods, it became obvious that a smaller degree of facial asymmetry is physiological, but if a certain threshold of asymmetry is exceeded, the face will be perceived as disfigured [32,33]. To determine whether a condition should be considered to be within the "normal range" or pathological, it became necessary to define methods to measure asymmetry in an objective and reproducible manner. To achieve this purpose, two methods have mainly been developed and used: first, the measurement of the position of characteristic points and their relation, and second, the measurement of distances of superimposed surfaces—an original one and a mirrored one.

The first method is commonly used in orthodontics, e.g., in the analysis of radiographs and casts. The advantage of this method is that it is possible to focus on a limited number of points, and the choice of landmarks can be used to focus on areas of interest and adapted to the phenomenon under examination. Where landmarks are not represented by eye-catching, well-defined structures, measuring points can be derived geometrically. Examples are the "Cranial Vault Asymmetry Index" (CVAI) [34] and the "Utrecht Cranial Shape Quantifier" (UCSQ) [35,36]. For the CVAI, two diagonal lines are drawn through the center of a horizontal head outline at a 30° angle to the median sagittal plane to both sides. The length of the two diagonal lines is related. Differences below 3.5% are regarded as normal (Figure 1).

The CVAI and comparable measurements of the head with mechanical measuring devices were evaluated and showed high intra- and inter-rater reliabilities [37]. Based on 3D radiographic data, the UCSQ uses four points (exocanthion and porion on both sides of the reconstructed skin surface). The left and right exocanthion and left porion define the basal plane. This plane is then shifted by 4 cm in the cranial direction. In these positions, the centroid of the reconstructed cross section of the skull and the distances and angles to the anterior and posterior and lateral outline points are measured. Based on the outline properties, a sinusoid curve is calculated.

Methods using landmarks for mirror plane localization and asymmetry quantification have been used with 2D photographs, 3D surface data and dental casts [38–41], and radiologic imaging such as panoramic radiographs, computed tomography (CT) scans and cone beam CT [42–44]. 3D techniques (CT and cone beam CT) should be given preference over panoramic radiographs, as the asymmetrical position of the skull will inevitably lead to asymmetric magnification factors. Using 3D data has the additional advantages of highly reliable symmetry plane detection and of adding the third dimension to asymmetry quantification. The combination of 3D surface data and CT data can facilitate the differentiation between skeletal and soft tissue asymmetries and their combination. The use of 3D surface data and Procrustes analysis for midsagittal plane detection is considered the gold standard for facial soft tissue asymmetry analysis [40].

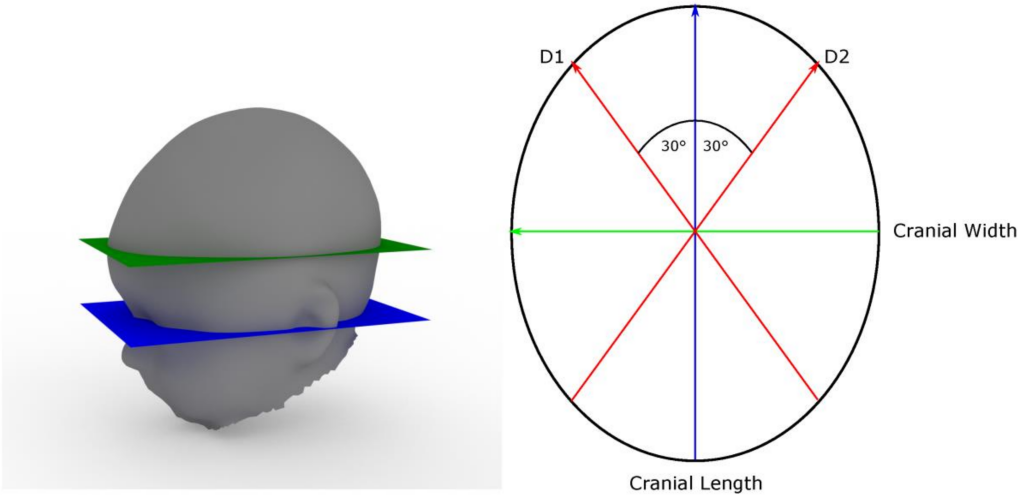


**Figure 1.** Calculation of the Cranial Vault Asymmetry Index (CVAI). (**Left**): A reference plane is defined by sellion and left and right tragion (blue). The plane is shifted vertically to the level of the largest anterior–posterior extension of the cranial length (green plane). (**Right**): At this level, the ratio of the length of two diagonal lines (D1 and D2) through the center of the cranial width (i.e., the line between the two tragi in the reference plane) at an angle of 30° to both sides of the cranial length (i.e., a line rectangular to the cranial width) is calculated using the formula $CVAI = |D1 - D2| / \max(D1, D2) \times 100$.

The second method used compares a surface with its mirrored counterpart. In contrast to using landmarks, there is no need to focus on a limited number of points. This method can be employed to localize and visualize areas of increased asymmetry. The method usually involves 3D surface data acquisition, mirroring of the surface and matching the surfaces via a best-fit algorithm [45–47]. For the latter purpose, the Iterative Closest Point algorithm (ICP) can be used [48]. With the superimposed surfaces, distance between corresponding points can be calculated automatically and transferred to a pseudocolor image. The mean distance between the corresponding points of the surfaces in relation to the size of the entire surface can be used as a simple measure of facial asymmetry, e.g., the Asymmetry Index (AI, Figure 2) [45,49].

A disadvantage of focusing on mean distances compared to the "landmark technique" is the fact that there is no correspondence to the process of visual perception in which facial contours are "tracked" by the observer, whose attention is attracted to certain regions of the face. Therefore, the mean distance between corresponding points might not necessarily correspond to perceived asymmetry. However, a correlation to subjective asymmetry estimation was shown [45]. Weighting these "eye-catching" areas of interest when calculating the asymmetry measure could even enhance the correlation between measured and perceived asymmetry. Reasonable approaches could be the weighting of the asymmetry calculation with the distance to the facial midline [50] or the distance to the edges of the Yarbus triangle, areas with high local mean curvature or the right side of the face.

Correlation between measured and perceived asymmetry can further be enhanced by weighting with the color difference $\Delta E$ between two corresponding contralateral points [49]. A low-contrast, fine-grained, randomly distributed texture, which is typical of older skin in particular, is evaluated as less attractive in itself, but this kind of color distribution is presumably not checked for symmetry [51,52]. It stands to reason that the perception of an asymmetrical color distribution depends strongly on the contrast and texture. Typical, high-contrast patterns such as Nevi naturally are perceived by their color, not by their shape. Their symmetrical arrangement is rather striking and judged less attractive than an asymmetrical appearance [50]. Perfect symmetry is said to be disconcerting [53,54]. However, artificially symmetrized photographs may include symmetry where it is an unexpected pattern, e.g., the hair falling over the forehead of the person depicted in the

photographs used by Silva et al. with a pair of absolutely symmetrical curls [55]. Therefore, the question still remains whether a face with perfect symmetry of the skin surface shape with naturally asymmetric hair and no Nevi would be rated less attractive than the same face with minor surface asymmetries.

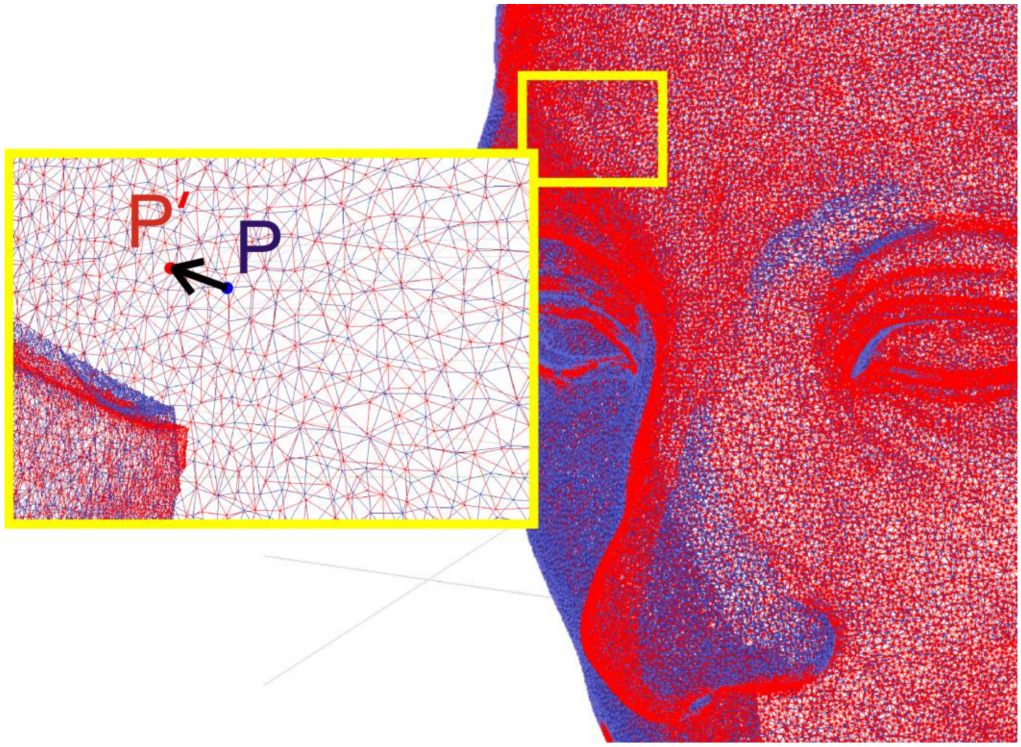


**Figure 2.** AI calculation [49] is based on the mean distance d of closest points between the original 3D surface (blue) and its mirrored and matched (registered) copy (red). In order to avoid scaling effects, it is divided by the frontal diagonal D of the bounding box enclosing the 3D surface. The corresponding formula is: $AI = d/D \times 1000$.

## 4. Symmetry of Teeth and Dental Arches

Mammalian molars evolved from simple, conical precursor forms (haplodontic) with one cusp (protocone) and one root, more or less rotationally or bilaterally symmetric. The triconodontic upper molar scheme shows two roots and three main cusps (paracone, protocone and metacone, with smaller additional cusps), in upper molars arranged more or less in a single row [56,57]. A triconodontic tooth scheme, therefore, shows bilateral symmetry to a frontal plane and to a sagittal plane. The three main cusps were rearranged from a line to a triangle in tritubercular molars [58]. With more complex tribosphenic teeth, simple schemes of bilateral symmetry were abandoned, mainly by the evolution of an additional main cusp, the hypocone [59]. However, at all stages of molar evolution, bilateral symmetry exists only to a limited degree of accuracy with smaller or larger deviations. There are still open questions in tooth morphogenesis and how genetic as well as environmental influences affect the localization of cuspal morphogenetic centers. Figure 3 shows patterns of dental symmetry of different evolutionary lines schematically. Figures 4 and 5 provide examples of the triconodontic and tribosphenic schemes, respectively.

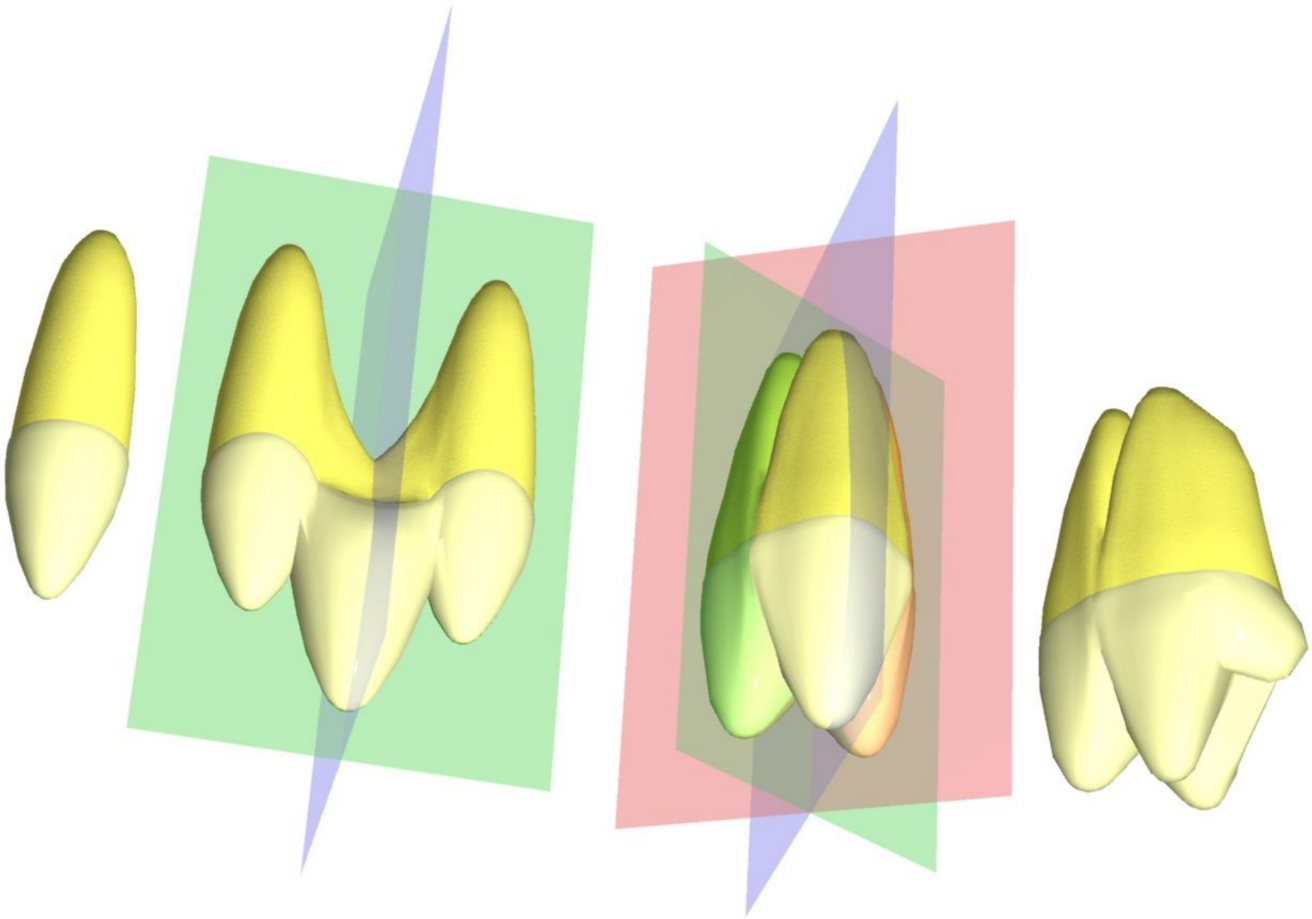

(**a**) (**b**) (**c**) (**d**)

**Figure 3.** Fundamental patterns of single upper right molar symmetry, from left to right: (**a**) radial symmetry of original conical, haplodont tooth with one cusp (protocone) and no occlusal surface; (**b**) triconodont scheme with three cusps (paracone, protocone and metacone) and two roots arranged in a line, exhibiting two symmetry planes; (**c**) tritubercular scheme with three roots and three cusps in a triangular arrangement. The rightmost scheme (**d**) is the tribosphenic one with an additional cusp (hypocone) as a major deviation from the three planes of bilateral symmetry of the tritubercular scheme.

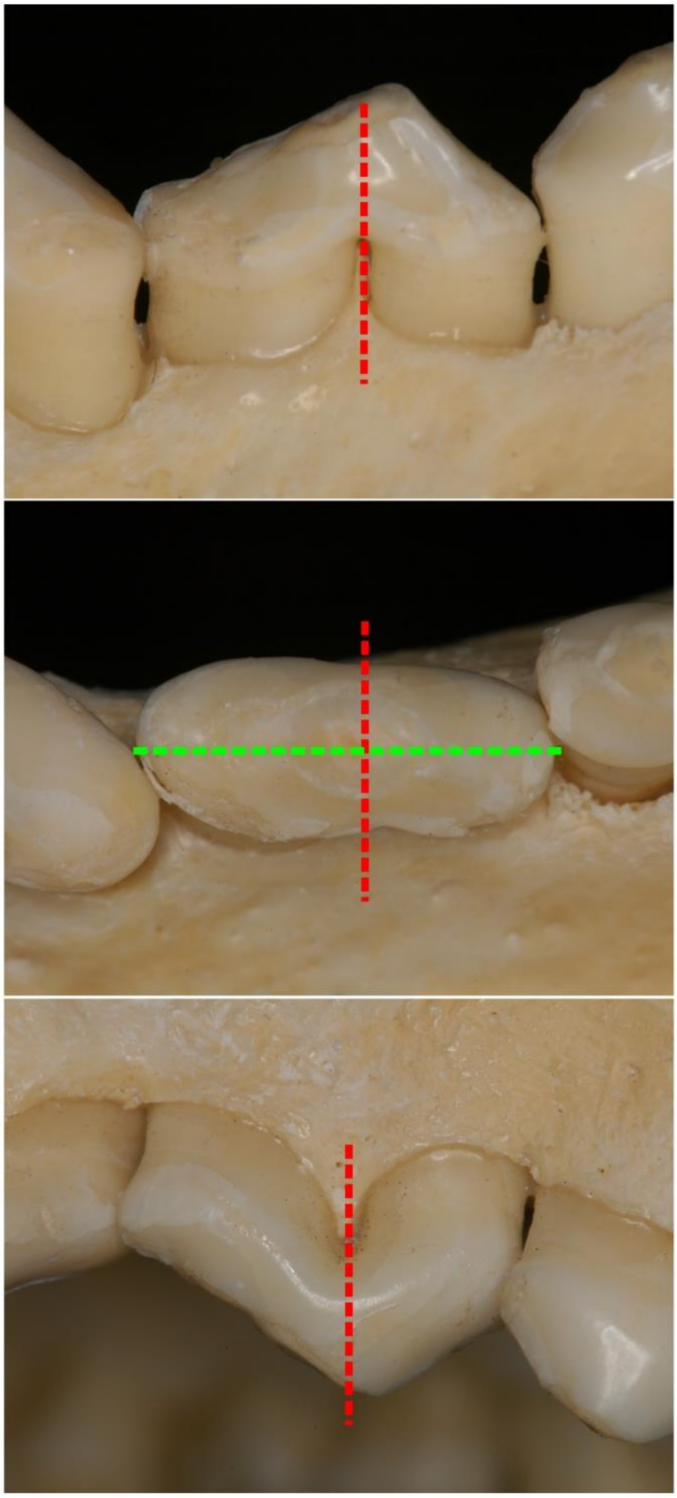

**Figure 4.** Upper right second premolar (P2) of *Canis lupus familiaris* following the triconodont scheme with two planes of bilateral symmetry indicated by dotted lines. (**Top**): view from palatal side. (**Center**): view from occlusal side. (**Bottom**): lateral view.

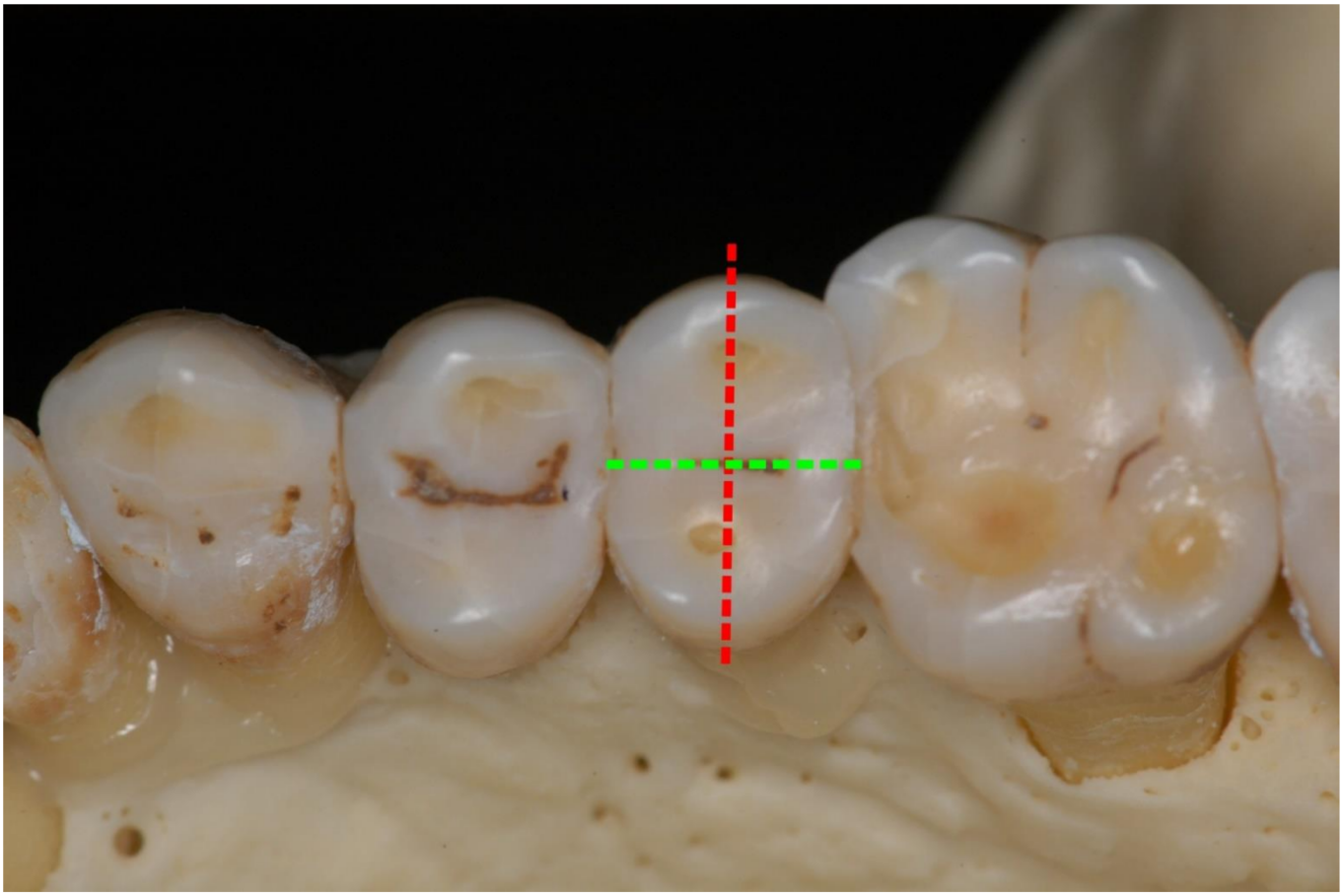

**Figure 5.** Human upper lateral teeth from canine to tribosphenic first molar. Dotted lines indicate symmetry planes of second premolar.

## 5. Bilateral Symmetry of Dental Arches and Jaws

The symmetry of single teeth has only a limited impact on health or dental therapy. In contrast, bilateral symmetry of the dental arches and certain structures may be of importance in orthodontic, endodontic and prosthodontic treatment as well as in maxillofacial surgery. For example, knowledge of root anatomy on one side might help in predicting the individual number of roots and root canals [60,61].

Felsypremila et al. reported bilateral symmetry concerning root and canal numbers between 81.5% of upper first and second premolar pairs (P1 and P2). With regard to first (M1) and second upper molars (M2), the corresponding proportions were 77.5% and 70.8%. In the lower jaw, the corresponding proportions of symmetrical forms were 96.1% (P1), 98.3% (P2) 78.6% (M1) and 70.8% (M2) [62].

Li et al. found very similar proportions in upper premolars (P1: 80.2%, P2: 81.8%) [63]. However, rare configurations of the roots and root canals occur much more frequently in an asymmetrical distribution [64].

There have been approaches to describe dental arch shape and symmetry using simple, symmetrical math formulas such as parabola and ellipse [65]. There have also been attempts to derive arch forms from a technical perspective, e.g., by understanding approximal contacts as overlapping dimeric link chains [66]. This approach would more or less force the dental arches into a predictable shape with only very limited influencing factors (shape of approximal surfaces). However, morphogenesis is a complex procedure influenced by the activity of morphogenes, epigenetic information, regulating factors and environmental conditions, including mechanical forces, as well as suppressing and reinforcing interactions of all these factors. Therefore, attempts to reduce the morphogenesis of dental arches to simplified mathematical models might be inappropriate.

Arches of healthy persons with full natural dentitions usually show only negligible asymmetry [67]. In malocclusion cases, dental and facial asymmetries are more frequently observed and more pronounced [68,69]. Asymmetry quantification of dental arches is usually performed using landmarks, as it gives an idea of the amount of orthodontic movement necessary to obtain symmetry [41,70].

Teeth and gingival tissues are visible during an expressive smile. The observer's attraction to the perioral region and the emotional signal of the smile has an important impact on attractiveness rating. Asymmetrical crown length and gingival height discrepancies and midline shifts were frequently examined. Most authors came to the conclusion that professionals, especially orthodontists, were more sensitive to asymmetrical changes than laypersons as far as crown length was concerned [23,71–76], though difference between laypersons and professionals was not significant in every study group. Anterior midline shifts of the upper central incisor midline in relation to the facial midline had a negative impact on the rated attractiveness at a discrepancy of 1 mm or more to the right and 2 mm or more to the left side, respectively [77]. Figure 6 shows a case with canine coronal height asymmetry and maxillary to mandibular midline shift.

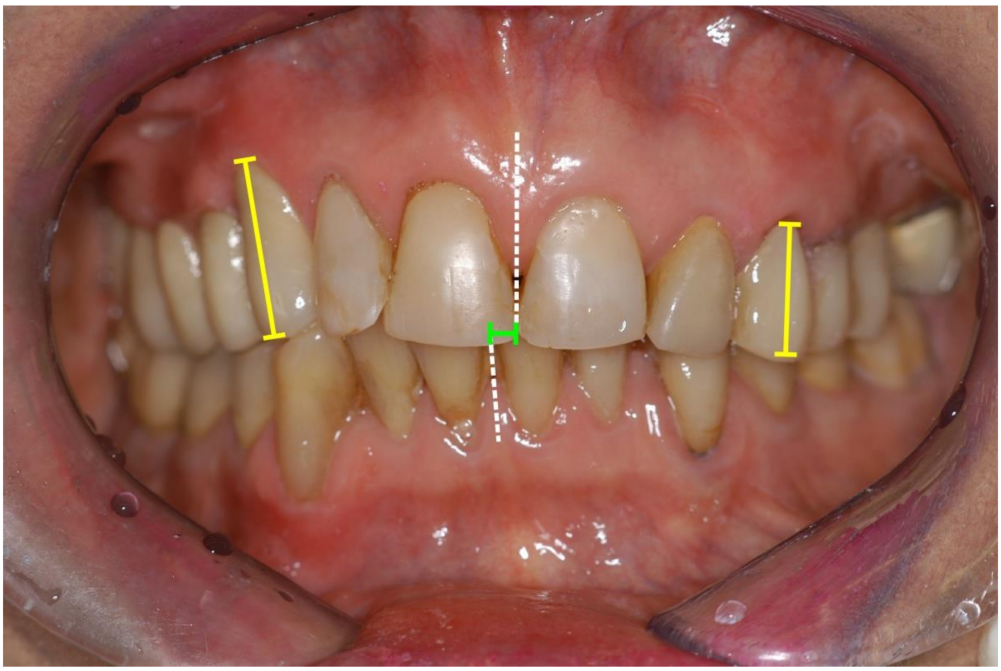

**Figure 6.** Anterior teeth of a 64-year-old female patient, exhibiting mandibular midline shift (green line), lower incisor angulation (white dotted lines) and crown height discrepancy between right and left incisors and canines (yellow lines). Treatment included surgical crown lengthening and crowns and fixed partial dentures from left canine to the left molar region. The patient's main concern was to improve her aesthetic appearance.

In more pronounced cases of unilateral malocclusions, adjustment, e.g., by orthodontic treatment, is recommended as they might not only be the reason for facial asymmetries, but also for temporomandibular disorders [78,79]. Recent studies indicate correlations between occlusion and adjacent structures including cervical spine, although the consequences of malocclusion and the success of treatment remain unanswered [80,81]. External and internal forces, e.g., by irregular tongue movements, can cause asymmetries of the dental arches [82]. With the introduction of dental implants as anchoring devices for orthodontic appliances, treatment options have been improved. Forces can more easily be applied only to unilateral segments of the dental arch without inducing a counterforce to the counterlateral teeth. In unilateral crossbite situations with insufficient width of the upper jaw, the unilateral mini-implant-assisted rapid palatal expander (U-MARPE, Figure 7) has been used successfully [83].

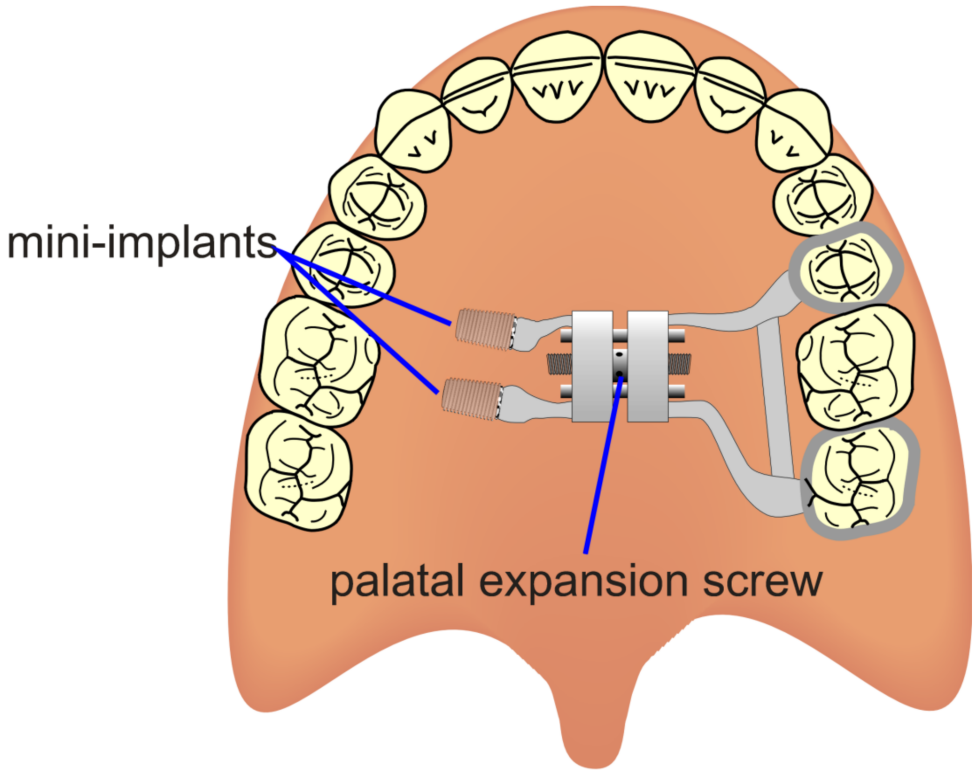


**Figure 7.** Unilateral mini-implant-assisted rapid palatal expander (U-MARPE [83]).

## 6. Congenital Structural Asymmetries of the Face

Asymmetric face clefts are among the most common congenital disorders with regionally varying prevalence [84]. Untreated unilateral cleft lips have a great impact on facial symmetry and even if successfully treated, cleft lip patients may exhibit asymmetry in perioral movements, e.g., when smiling [85]. Other structural asymmetries include missing teeth and teeth disproportions with smaller teeth on the affected side of the maxilla, although mandibular teeth were larger on the cleft side and dental asymmetries also occur in unaffected persons [86–89].

Thierens et al. used landmark-based 2D analysis as well as 3D superimposed labial and nasal surfaces to evaluate treatment results after autologous bone grafting in 15 unilateral cleft lip patients [90]. Significant improvements could only be demonstrated with the landmark-based 2D technique, showing a reduction in the affected/healthy side ratio of the distance from midline to lateral labial commissure, meaning the labial commissures were more symmetrical after treatment. However, 3D surface asymmetry quantification technology has also been successfully used to examine cleft lip and palate patients before and after treatment and to evaluate treatment success with different methods [91].

Craniofacial malformations caused by synostoses and pharyngeal arch syndromes are less common, but can lead to severe proportional disfigurements of the head and face, including asymmetries. The extent of malformation and asymmetry can vary widely and affect both hard and soft facial tissues [92]. Examples are Treacher Collins, Crouzon, Apert, Pfeiffer and Saethre-Chotzen syndrome [93–95]. A large number of gene mutations have been found to be related to craniosynostoses, e.g., mutations of the TWIST1 gene on chromosome 7p21.1 in the case of Saethre-Chotzen syndrome. However, environmental factors are also of importance for the development of these rare diseases [96,97]. Affected persons may suffer from severe consequences and dysfunctions, e.g., encephaloceles, hypertelorism, anterior open bite, temporomandibular joint malformations and airway obstructions [95,98,99]. Parental acceptance and the development of self-concept and social competence may be affected and should be taken into consideration as well [100], indepen-

dent from the question of whether a facial malformation is exhibited in a symmetrical or an asymmetrical pattern.

Treatment should be performed by experienced maxillofacial surgeons and neurosurgeons and includes resection, rearrangement and replacement of craniofacial structures, e.g., fronto-orbital or frontofacial advancement in Pfeiffer, Apert and Crouzon syndrome [101,102]. Lambdoid synostosis leads to a condition very similar to plagiocephaly and distinguishing the two conditions is a diagnostic challenge [103,104]. In contrast to synostoses, plagiocephaly is caused by external forces and can be treated by helmet therapy. Hemifacial microsomia and Goldenhar syndrome are examples of malformations originating from the first pharyngeal arch. As the term hemifacial microsomia indicates, structures of the face including forebrain and eye, ear and mandible may be affected in an asymmetrical pattern. However, in spite of its name, hemifacial microsomia affects both sides of an asymmetrically distributed extent. The cause of the disease is suspected to be a genetic defect on chromosome 14 [105]. The chin is displaced asymmetrically to the more affected side and anterior open bite is a frequent consequence. Teeth size [106] is reduced in the affected region, but more severe are the consequences of an unilaterally hypoplastic temporomandibular joint. Because of the different severity and prognosis, hemifacial microsomia has to be distinguished from hemimandibular hypoplasia [107,108]. Treatment includes surgical symmetrization by artificial joints and corrections of the facial shape with autologous fat flaps [109–111]. Less severe cases can be treated orthognathically [112]. Therapy again primarily includes maxillofacial surgery, usually in combination with orthodontic treatment and is eventually supported by interocclusal splints and prosthodontics. Within the last few decades, distraction osteogenesis has enriched the spectrum of therapy [113,114].

Unilateral facial port-wine stain is another congenital asymmetry, but without major macroscopic, structural malformations. Treatment is nevertheless mandatory to restore facial aesthetics [115].

## 7. Acquired Structural and Functional Asymmetries of the Head and Face

Acquired structural asymmetry includes trauma, neoplastic diseases and infections. Infectious diseases such as Noma [116–118] and facial skin tuberculosis [119] have been a common cause of facial disfigurement and still occur. Today, disfiguring infections of the facial soft tissues can successfully be prevented by avoiding predisposing factors such as malnutrition or can be treated with antibiotics.

However, neoplastic diseases, especially head and neck cancer, and facial trauma are seen much more frequently today. Squamous cell carcinoma within the oral cavity is often diagnosed by dentists. Treatment includes maxillofacial surgery and radiation therapy. The primary goal of therapy is complete resection of the tumor tissue. Facial asymmetry after tumor resection is often unavoidable as a direct or indirect consequence of substance loss. Reconstructive surgery in the treatment of craniofacial defects can be performed using autologous bone and flaps or allogeneic material such as titanium or Polyether ether ketone (PEEK) [120–122].

Partial mandibular resection with complete transection of the mandibular bone without reconstruction will lead to mandibular dislocation and functional asymmetry (Figures 8 and 9). Radiation and scarring may even increase structural and functional asymmetry. Therefore, surgical reconstruction of the mandible is the therapy of choice whenever it is possible [123].

(**a**) (**b**)

**Figure 8.** Anteroposterior radiograph (**a**) and aspect of a male patient (**b**) suffering from oral cancer of the tongue and mandible. After tumor surgery and radiation therapy, the mandibular bones were connected by a reconstruction plate. Following local infection, reconstruction was no longer possible and, therefore, a gap between the right and left mandible remains on the patient's left side (red dotted lines). Arrows indicate upper and lower jaw midline.

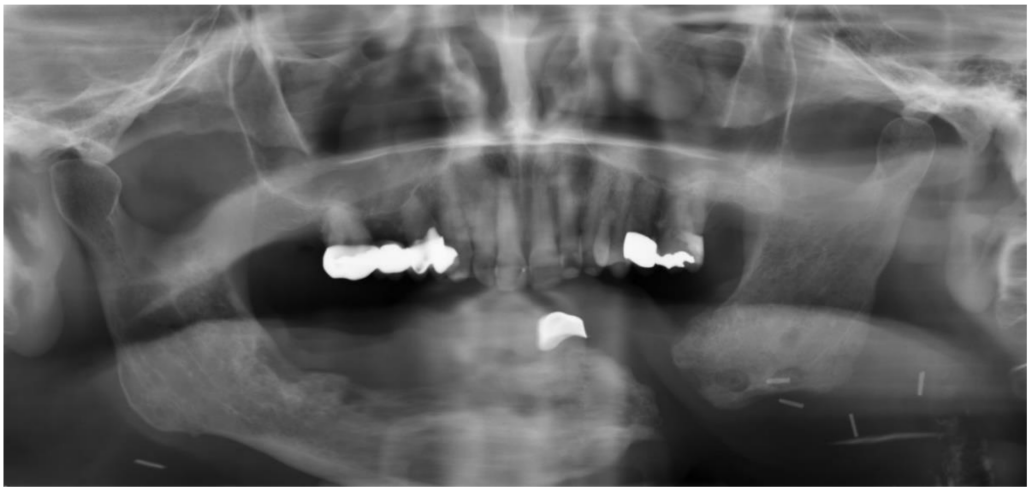

**Figure 9.** Panoramic radiograph of the same patient three years later after further tooth loss.

Unilateral mandibular condylar hyperplasia is a rare disease, where one condyle exhibits excessive growth [124–126]. A benign tumor of the long bones, osteochondroma, may also affect the mandibular condyle with similar consequences: Condylar growth leads to dislocation of the mandibular body in vertical and/or anterior direction. Asymmetry and occlusal imbalances are frequent consequences (Figures 10 and 11). Treatment includes surgical remodeling or removal of the affected condyle and, if necessary, insertion of a neocondyle.

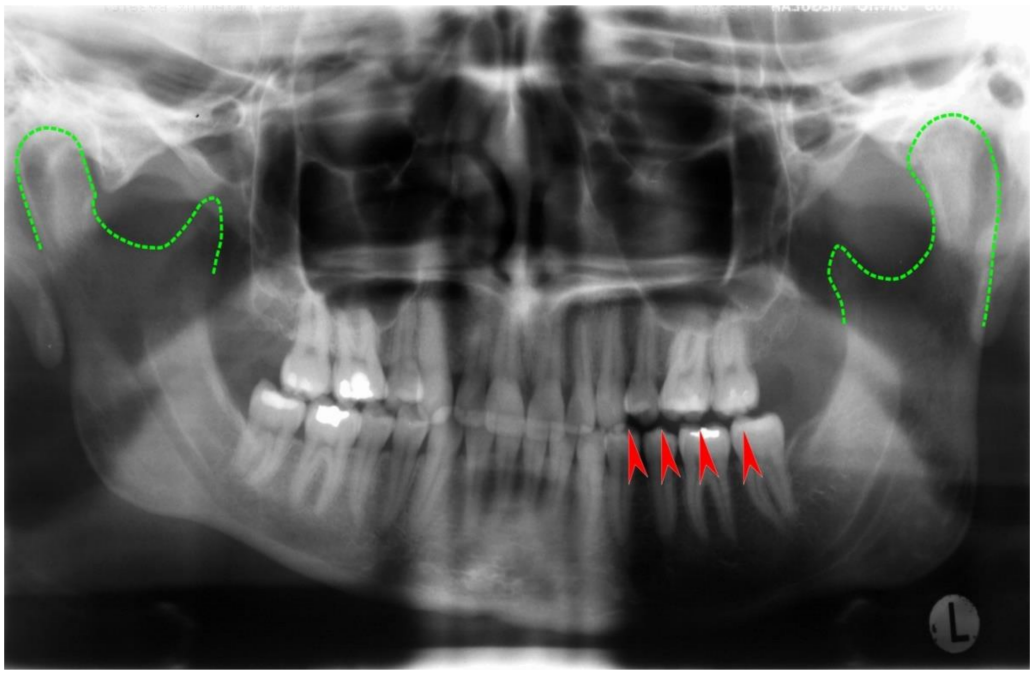

**Figure 10.** Panoramic radiograph of a unilateral condylar hyperplasia on a 38-year-old female patient's left side. Green dotted lines outline the condyles; arrows indicate non-occlusion in the left bicuspid and molar region. In this case, the panoramic radiograph gives an impression of asymmetry. However, CT and cone beam CT are superior in accuracy.

**Figure 11.** Intraoral view of the same patient. Unilateral open bite on the left side and moderate mandibular midline shift are clearly visible. At present, occlusal stability is maintained by an intraoral splint until a definite correction with crowns and overlays in the left mandible will be performed.

CAD-CAM technology has greatly improved surgical procedures, prosthodontics and maxillofacial prosthetics [127]. The shape and effects of alloplastic implants can be planned with 3D models [120]. Facial prostheses for defects after resection of the eye and periorbital tissues can be planned and evaluated using facial scans and registration with a best-fit algorithm [128–130]. As face scans can be related to intraoral structures and devices [131],

the symmetry plane of the face can be correlated to the symmetry plane of a planned dental prosthesis [132].

Unilateral facial paralysis leads to asymmetry either at rest or in motion. The consequences range from a mask-like facial expression to inflammation of the eye and conjunctiva and difficulty in speaking, swallowing, eating and drinking to a reduced quality of life and depression [133]. Treatment options depend on the cause of the disorder and include neurosurgical nerve reconstruction [134], plastic surgery [135], contralateral botulinum toxin injections [136–138] and even cheek, lip and labial commissure supporting dental appliances [139,140].

## 8. Conclusions

Asymmetry of the head, especially of the face, is a condition with more or less severe consequences on orofacial function and facial appearance. The subjective burden of physical and psychosocial implications can vary greatly from person to person. To obtain an objective assessment of the severity of facial asymmetry, a thorough understanding of the processes of perception of faces and the normal range is necessary. For a successful therapy, the precise detection and localization of regional asymmetries are prerequisites. Supported by 3D data acquisition using optical surface scan technology or three-dimensional radiographs, analysis and quantification of asymmetries can be performed more precisely today. This development will probably continue enhancing surgical, orthodontic and prosthodontic treatment planning and implementation, e.g., by merging diagnostic 3D data from different sources with dental CAD-CAM technologies.

**Author Contributions:** Conceptualization: C.R. and D.D.; software: D.D.; writing—original draft prepararion: C.R.; writing—review and editing: C.R. and D.D. All authors have read and agreed to the published version of the manuscript.

**Funding:** This research received no external funding.

**Informed Consent Statement:** Written informed consent has been obtained from the patients to publish this paper.

**Conflicts of Interest:** The authors declare no conflict of interest.

## References

1. Li, Y.; Omori, A.; Flores, R.L.; Satterfield, S.; Nguyen, C.; Ota, T.; Tsurugaya, T.; Ikuta, T.; Ikeo, K.; Kikuchi, M.; et al. Genomic insights of body plan transitions from bilateral to pentameral symmetry in Echinoderms. *Commun. Biol.* **2020**, *3*, 371. [CrossRef]
2. Harrington, R.C.; Faircloth, B.C.; Eytan, R.I.; Smith, W.L.; Near, T.J.; Alfaro, M.E.; Friedman, M. Phylogenomic analysis of carangimorph fishes reveals flatfish asymmetry arose in a blink of the evolutionary eye. *BMC Evol. Biol.* **2016**, *16*, 224. [CrossRef]
3. Marks, S.C.; Gorski, J.P.; Wise, G.E. The mechanisms and mediators of tooth eruption—Models for developmental biologists. *Int. J. Dev. Biol.* **1995**, *39*, 223–230.
4. Maltha, J.C. Mechanismen van tanderuptie. *Ned. Tijdschr. Tandheelkd.* **2014**, *121*, 209–214. [CrossRef] [PubMed]
5. Wise, G.E.; Frazier-Bowers, S.; D'Souza, R.N. Cellular, molecular, and genetic determinants of tooth eruption. *Crit. Rev. Oral Biol. Med.* **2002**, *13*, 323–334. [CrossRef]
6. Starcke, E.N. The history of articulators: A critical history of articulators based on "geometric" theories of mandibular movement. Part IV: Needles, Wadsworth, and a look at some who followed. *J. Prosthodont.* **2003**, *12*, 51–62. [CrossRef]
7. Wurtz, R.H. Recounting the impact of Hubel and Wiesel. *J. Physiol.* **2009**, *587*, 2817–2823. [CrossRef]
8. Hubel, D.; Wiesel, T. David Hubel and Torsten Wiesel. *Neuron* **2012**, *75*, 182–184. [CrossRef]
9. Larsson, J.; Landy, M.S.; Heeger, D.J. Orientation-selective adaptation to first- and second-order patterns in human visual cortex. *J. Neurophysiol.* **2006**, *95*, 862–881. [CrossRef]
10. Baldwin, M.K.L.; Balaram, P.; Kaas, J.H. The evolution and functions of nuclei of the visual pulvinar in primates. *J. Comp. Neurol.* **2017**, *525*, 3207–3226. [CrossRef]
11. Yarbus, A.L. *Eye Movements and Vision*; Springer: Boston, MA, USA, 1967; ISBN 978-1-4899-5381-0.
12. Sadr, J.; Krowicki, L. Face perception loves a challenge: Less information sparks more attraction. *Vis. Res.* **2019**, *157*, 61–83. [CrossRef]
13. Halit, H.; de Haan, M.; Schyns, P.G.; Johnson, M.H. Is high-spatial frequency information used in the early stages of face detection? *Brain Res.* **2006**, *1117*, 154–161. [CrossRef]

14. Blaisdell, A.P. Mental imagery in animals: Learning, memory, and decision-making in the face of missing information. *Learn. Behav.* **2019**, *47*, 193–216. [CrossRef]
15. Mertens, I.; Siegmund, H.; Grüsser, O.-J. Gaze motor asymmetries in the perception of faces during a memory task. *Neuropsychologia* **1993**, *31*, 989–998. [CrossRef]
16. Guo, K.; Smith, C.; Powell, K.; Nicholls, K. Consistent left gaze bias in processing different facial cues. *Psychol. Res.* **2012**, *76*, 263–269. [CrossRef] [PubMed]
17. Kramer, R.S.S.; Ward, R. Different signals of personality and health from the two sides of the face. *Perception* **2011**, *40*, 549–562. [CrossRef]
18. Meyer-Marcotty, P.; Stellzig-Eisenhauer, A.; Bareis, U.; Hartmann, J.; Kochel, J. Three-dimensional perception of facial asymmetry. *Eur. J. Orthod.* **2011**, *33*, 647–653. [CrossRef]
19. Chu, E.A.; Farrag, T.Y.; Ishii, L.E.; Byrne, P.J. Threshold of visual perception of facial asymmetry in a facial paralysis model. *Arch. Facial Plast. Surg.* **2011**, *13*, 14–19. [CrossRef]
20. Hohman, M.H.; Kim, S.W.; Heller, E.S.; Frigerio, A.; Heaton, J.T.; Hadlock, T.A. Determining the threshold for asymmetry detection in facial expressions. *Laryngoscope* **2014**, *124*, 860–865. [CrossRef]
21. Zamanian, N.; Jafari-Naeimi, A. The Perception of the Severity of Facial Asymmetry among Laypersons, General Practitioners, Orthodontists, and Maxillofacial Surgeons. *J. Dent.* **2021**, *22*, 102–108. [CrossRef]
22. Bispo de Carvalho Barbosa, P.; de Andrade Vieira, W.; de Macedo Bernardino, Í.; Costa, M.M.; Pithon, M.M.; Paranhos, L.R. Aesthetic facial perception and need for treatment in simulated laterognathism in male faces of different ethnicities. *Oral Maxillofac. Surg.* **2019**, *23*, 407–413. [CrossRef]
23. Kokich, V.O.; Kokich, V.G.; Kiyak, H.A. Perceptions of dental professionals and laypersons to altered dental esthetics: Asymmetric and symmetric situations. *Am. J. Orthod. Dentofac. Orthop.* **2006**, *130*, 141–151. [CrossRef]
24. Kim, S.W.; Heller, E.S.; Hohman, M.H.; Hadlock, T.A.; Heaton, J.T. Detection and perceptual impact of side-to-side facial movement asymmetry. *JAMA Facial Plast. Surg.* **2013**, *15*, 411–416. [CrossRef]
25. Bradbury, E. Meeting the psychological needs of patients with facial disfigurement. *Br. J. Oral Maxillofac. Surg.* **2012**, *50*, 193–196. [CrossRef]
26. Thompson, A.; Kent, G. Adjusting to disfigurement: Processes involved in dealing with being visibly different. *Clin. Psychol. Rev.* **2001**, *21*, 663–682. [CrossRef]
27. Macgregor, F.C. Facial disfigurement: Problems and management of social interaction and implications for mental health. *Aesthetic Plast. Surg.* **1990**, *14*, 249–257. [CrossRef]
28. Shanmugarajah, K.; Gaind, S.; Clarke, A.; Butler, P.E.M. The role of disgust emotions in the observer response to facial disfigurement. *Body Image* **2012**, *9*, 455–461. [CrossRef] [PubMed]
29. van den Elzen, M.E.P.; Versnel, S.L.; Hovius, S.E.R.; Passchier, J.; Duivenvoorden, H.J.; Mathijssen, I.M.J. Adults with congenital or acquired facial disfigurement: Impact of appearance on social functioning. *J. Craniomaxillofac. Surg.* **2012**, *40*, 777–782. [CrossRef]
30. Higgins, E.T. Self-discrepancy: A theory relating self and affect. *Psychol. Rev.* **1987**, *94*, 319–340. [CrossRef] [PubMed]
31. Dürer, A. Hierinn Sind Begriffen Vier Bucher Von Menschlicher Proportion Durch Albrechten Durer von Nurerberg [sic.] Erfunden Und Beschuben Zu Nutz Allen Denen So Zu Diser Kunst Lieb Tragen. *Eye Movements and Vision*; Hieronymus Andreae Formschneider: Nuremberg, Germany, 1528. Available online: https://archive.org/details/hierinnsindbegri00dure/page/54/mode/2up (accessed on 30 June 2021).
32. Kobus, K.; Kobus-Zaleśna, K. The treatment of facial asymmetry: Review. *Adv. Clin. Exp. Med.* **2017**, *26*, 1301–1311. [CrossRef]
33. Wang, T.T.; Wessels, L.; Hussain, G.; Merten, S. Discriminative Thresholds in Facial Asymmetry: A Review of the Literature. *Aesthet. Surg. J.* **2017**, *37*, 375–385. [CrossRef]
34. Loveday, B.P.; Chalain, T.B. de. Active counterpositioning or orthotic device to treat positional plagiocephaly? *J. Craniofac. Surg.* **2001**, *12*, 308–313. [CrossRef]
35. Kronig, O.D.M.; Kronig, S.A.J.; Vrooman, H.A.; Veenland, J.F.; Jippes, M.; Boen, T.; van Adrichem, L.N.A. Introducing a new method for classifying skull shape abnormalities related to craniosynostosis. *Eur. J. Pediatr.* **2020**, *179*, 1569–1577. [CrossRef] [PubMed]
36. Kronig, S.A.J.; Kronig, O.D.M.; Vrooman, H.A.; Veenland, J.F.; van Adrichem, L.N.A. Quantification of Severity of Unilateral Coronal Synostosis. *Cleft Palate Craniofac. J.* **2021**, *58*, 832–837. [CrossRef]
37. Pastor-Pons, I.; Lucha-López, M.O.; Barrau-Lalmolda, M.; Rodes-Pastor, I.; Rodríguez-Fernández, Á.L.; Hidalgo-García, C.; Tricás-Moreno, J.M. Interrater and Intrarater Reliability of Cranial Anthropometric Measurements in Infants with Positional Plagiocephaly. *Children* **2020**, *7*, 306. [CrossRef] [PubMed]
38. Berssenbrügge, P.; Berlin, N.F.; Kebeck, G.; Runte, C.; Jung, S.; Kleinheinz, J.; Dirksen, D. 2D and 3D analysis methods of facial asymmetry in comparison. *J. Craniomaxillofac. Surg.* **2014**, *42*, e327–e334. [CrossRef] [PubMed]
39. Berlin, N.F.; Berssenbrügge, P.; Runte, C.; Wermker, K.; Jung, S.; Kleinheinz, J.; Dirksen, D. Quantification of facial asymmetry by 2D analysis—A comparison of recent approaches. *J. Craniomaxillofac. Surg.* **2014**, *42*, 265–271. [CrossRef] [PubMed]
40. Damstra, J.; Fourie, Z.; de Wit, M.; Ren, Y. A three-dimensional comparison of a morphometric and conventional cephalometric midsagittal planes for craniofacial asymmetry. *Clin. Oral Investig.* **2012**, *16*, 285–294. [CrossRef] [PubMed]
41. Ferrario, V.F.; Sforza, C.; Miani, A.; Serrao, G. Dental arch asymmetry in young healthy human subjects evaluated by Euclidean distance matrix analysis. *Arch. Oral Biol.* **1993**, *38*, 189–194. [CrossRef]

42. Boratto, R.; Gambardella, U.; Micheletti, P.; Pagliani, L.; Preda, L.; Hansson, T.L. Condylar-mandibular asymmetry, a reality. *Bull. Group. Int. Rech. Sci. Stomatol. Odontol.* **2002**, *44*, 52–56.
43. van Elslande, D.C.; Russett, S.J.; Major, P.W.; Flores-Mir, C. Mandibular asymmetry diagnosis with panoramic imaging. *Am. J. Orthod. Dentofac. Orthop.* **2008**, *134*, 183–192. [CrossRef]
44. Sanders, D.A.; Chandhoke, T.K.; Uribe, F.A.; Rigali, P.H.; Nanda, R. Quantification of skeletal asymmetries in normal adolescents: Cone-beam computed tomography analysis. *Prog. Orthod.* **2014**, *15*, 26. [CrossRef] [PubMed]
45. Ostwald, J.; Berssenbrügge, P.; Dirksen, D.; Runte, C.; Wermker, K.; Kleinheinz, J.; Jung, S. Measured symmetry of facial 3D shape and perceived facial symmetry and attractiveness before and after orthognathic surgery. *J. Craniomaxillofac. Surg.* **2015**, *43*, 521–527. [CrossRef] [PubMed]
46. Ekrami, O.; Claes, P.; White, J.D.; Zaidi, A.A.; Shriver, M.D.; van Dongen, S. Measuring asymmetry from high-density 3D surface scans: An application to human faces. *PLoS ONE* **2018**, *13*, e0207895. [CrossRef]
47. Zhu, Y.; Zheng, S.; Yang, G.; Fu, X.; Xiao, N.; Wen, A.; Wang, Y.; Zhao, Y. A novel method for 3D face symmetry reference plane based on weighted Procrustes analysis algorithm. *BMC Oral Health* **2020**, *20*, 319. [CrossRef] [PubMed]
48. Besl, P.J.; McKay, N.D. Method for registration of 3-D shapes. In Proceedings of the SPIE—The International Society for Optical Engineering, Orlando, FL, USA, 25–29 October 1992; Volume 14, pp. 586–606. [CrossRef]
49. Berssenbrügge, P.; Lingemann-Koch, M.; Abeler, A.; Runte, C.; Jung, S.; Kleinheinz, J.; Denz, C.; Dirksen, D. Measuring facial symmetry: A perception-based approach using 3D shape and color. *Biomed. Tech.* **2015**, *60*, 39–47. [CrossRef]
50. Springer, I.N.; Wannicke, B.; Warnke, P.H.; Zernial, O.; Wiltfang, J.; Russo, P.A.J.; Terheyden, H.; Reinhardt, A.; Wolfart, S. Facial attractiveness: Visual impact of symmetry increases significantly towards the midline. *Ann. Plast. Surg.* **2007**, *59*, 156–162. [CrossRef]
51. Matts, P.J.; Fink, B.; Grammer, K.; Burquest, M. Color homogeneity and visual perception of age, health, and attractiveness of female facial skin. *J. Am. Acad. Dermatol.* **2007**, *57*, 977–984. [CrossRef]
52. Fink, B.; Matts, P.J.; Klingenberg, H.; Kuntze, S.; Weege, B.; Grammer, K. Visual attention to variation in female facial skin color distribution. *J. Cosmet. Dermat.* **2008**, *7*, 155–161. [CrossRef]
53. Swaddle, J.P.; Cuthill, I.C. Asymmetry and human facial attractiveness: Symmetry may not always be beautiful. *Proc. Biol. Sci.* **1995**, *261*, 111–116. [CrossRef]
54. Scheuerle, A.E.; Firth, R.M. Asymmetric faces: Symbolic, spiritual, and representative. *Am. J. Med. Genet. C Semin. Med. Genet.* **2021**, *187*, 278–282. [CrossRef]
55. Silva, B.P.; Jiménez-Castellanos, E.; Martinez-de-Fuentes, R.; Greenberg, J.R.; Chu, S. Laypersons' perception of facial and dental asymmetries. *Int. J. Periodontics Restor. Dent.* **2013**, *33*, e162–e171. [CrossRef]
56. Jäger, K.R.K.; Cifelli, R.L.; Martin, T. Molar occlusion and jaw roll in early crown mammals. *Sci. Rep.* **2020**, *10*, 22378. [CrossRef]
57. Sulej, T.; Krzesiński, G.; Tałanda, M.; Wolniewicz, A.S.; Błażejowski, B.; Bonde, N.; Gutowski, P.; Sienkiewicz, M.; Niedźwiedzki, G. The earliest-known mammaliaform fossil from Greenland sheds light on origin of mammals. *Proc. Natl. Acad. Sci. USA* **2020**, *117*, 26861–26867. [CrossRef]
58. Couzens, A.M.C.; Sears, K.E.; Rücklin, M. Developmental influence on evolutionary rates and the origin of placental mammal tooth complexity. *Proc. Natl. Acad. Sci. USA* **2021**, *118*, e2019294118. [CrossRef]
59. Hunter, J.P.; Jernvall, J. The hypocone as a key innovation in mammalian evolution. *Proc. Natl. Acad. Sci. USA* **1995**, *92*, 10718–10722. [CrossRef]
60. Alghamdi, F.T.; Khalil, W.A. Root canal morphology and symmetry of mandibular second premolars using cone-beam computed tomography. *Oral Radiol.* **2021**, 1–13, Online ahead of print. [CrossRef]
61. Bürklein, S.; Heck, R.; Schäfer, E. Evaluation of the Root Canal Anatomy of Maxillary and Mandibular Premolars in a Selected German Population Using Cone-beam Computed Tomographic Data. *J. Endod.* **2017**, *43*, 1448–1452. [CrossRef]
62. Felsypremila, G.; Vinothkumar, T.S.; Kandaswamy, D. Anatomic symmetry of root and root canal morphology of posterior teeth in Indian subpopulation using cone beam computed tomography: A retrospective study. *Eur. J. Dent.* **2015**, *9*, 500–507. [CrossRef]
63. Li, Y.-H.; Bao, S.-J.; Yang, X.-W.; Tian, X.-M.; Wei, B.; Zheng, Y.-L. Symmetry of root anatomy and root canal morphology in maxillary premolars analyzed using cone-beam computed tomography. *Arch. Oral Biol.* **2018**, *94*, 84–92. [CrossRef]
64. Kantilieraki, E.; Delantoni, A.; Angelopoulos, C.; Beltes, P. Evaluation of Root and Root Canal Morphology of Mandibular First and Second Molars in a Greek Population: A CBCT Study. *Eur. Endod. J.* **2019**, *4*, 62–68. [CrossRef]
65. Pokhariyal, G.P.; Moturi, C.A.; Hassanali, J.; Kinyanjui, S.M. Simulation model for dental arch shapes. *East Afr. Med. J.* **2004**, *81*, 599–602. [PubMed]
66. Ihlow, D.; Kubein-Meesenburg, D.; Hunze, J.; Dathe, H.; Planert, J.; Schwestka-Polly, R.; Nägerl, H. Curvature morphology of the mandibular dentition and the development of concave-convex vertical stripping instruments. *J. Orofac. Orthop.* **2002**, *63*, 274–282. [CrossRef]
67. Al-Zubair, N.M. Dental arch asymmetry. *Eur. J. Dent.* **2014**, *8*, 224–228. [CrossRef] [PubMed]
68. Nie, Q.; Lin, J. Analysis and comparison of dental arch symmetry between different Angle's malocclusion categories and normal occlusion. *Zhonghua Kou Qiang Yi Xue Za Zhi* **2000**, *35*, 105–107. [PubMed]
69. Uysal, T.; Kurt, G.; Ramoglu, S.I. Dental and alveolar arch asymmetries in normal occlusion and Class II Division 1 and Class II subdivision malocclusions. *World J. Orthod.* **2009**, *10*, 7–15.

70. Ferrario, V.F.; Sforza, C.; Colombo, A.; Miani, A.; D'Addona, A. Position and asymmetry of teeth in untreated dental arches. *Int. J. Adult Orthodon. Orthognath. Surg.* **1993**, *8*, 277–285.
71. Kumar, S.; Gandhi, S.; Valiathan, A. Perception of smile esthetics among Indian dental professionals and laypersons. *Indian J. Dent. Res.* **2012**, *23*, 295. [CrossRef]
72. Thomas, M.; Reddy, R.; Reddy, B.J. Perception differences of altered dental esthetics by dental professionals and laypersons. *Indian J. Dent. Res.* **2011**, *22*, 242–247. [CrossRef]
73. Katiyar, S.; Gandhi, S.; Sodawala, J.; Anita, G.; Hamdani, S.; Jain, S. Influence of symmetric and asymmetric alterations of maxillary canine gingival margin on the perception of smile esthetics among orthodontists, dentists, and laypersons. *Indian J. Dent. Res.* **2016**, *27*, 586–591. [CrossRef]
74. Pinho, S.; Ciriaco, C.; Faber, J.; Lenza, M.A. Impact of dental asymmetries on the perception of smile esthetics. *Am. J. Orthod. Dentofac. Orthop.* **2007**, *132*, 748–753. [CrossRef]
75. Correa, B.D.; Vieira Bittencourt, M.A.; Machado, A.W. Influence of maxillary canine gingival margin asymmetries on the perception of smile esthetics among orthodontists and laypersons. *Am. J. Orthod. Dentofac. Orthop.* **2014**, *145*, 55–63. [CrossRef]
76. Lauria, A.; Rodrigues, D.C.; de Medeiros, R.C.; Moreira, R.W.F. Perception of oral and maxillofacial surgeons, orthodontists and laypersons in relation to the harmony of the smile. *J. Craniomaxillofac. Surg.* **2014**, *42*, 1664–1668. [CrossRef]
77. Silva, B.P.; Jiménez-Castellanos, E.; Martinez-de-Fuentes, R.; Fernandez, A.A.V.; Chu, S. Perception of maxillary dental midline shift in asymmetric faces. *Int. J. Esthet. Dent.* **2015**, *10*, 588–596. [PubMed]
78. Thilander, B.; Lennartsson, B. A study of children with unilateral posterior crossbite, treated and untreated, in the deciduous dentition–occlusal and skeletal characteristics of significance in predicting the long-term outcome. *J. Orofac. Orthop.* **2002**, *63*, 371–383. [CrossRef] [PubMed]
79. Gesch, D.; Bernhardt, O.; Alte, D.; Kocher, T.; John, U.; Hensel, E. Malocclusions and clinical signs or subjective symptoms of temporomandibular disorders (TMD) in adults. Results of the population-based Study of Health in Pomerania (SHIP). *J. Orofac. Orthop.* **2004**, *65*, 88–103. [CrossRef] [PubMed]
80. Cardinal, L.; Da Silva, T.R.; Andujar, A.L.F.; Gribel, B.F.; Dominguez, G.C.; Janakiraman, N. Evaluation of the three-dimensional (3D) position of cervical vertebrae in individuals with unilateral posterior crossbite. *Clin. Oral Investig.* **2021**, *13*, 1–7. [CrossRef]
81. Melink, S.; Vagner, M.V.; Hocevar-Boltezar, I.; Ovsenik, M. Posterior crossbite in the deciduous dentition period, its relation with sucking habits, irregular orofacial functions, and otolaryngological findings. *Am. J. Orthod. Dentofac. Orthop.* **2010**, *138*, 32–40. [CrossRef] [PubMed]
82. Ovsenik, M.; Primožič, J. Repousser les limites de la dimension transversale. Asymétrie faciale, volume du palais et posture linguale chez les enfants ayant une occlusion croisée unilatérale postérieure: Évaluation tridimensionnelle d'un traitement précoce. *Orthod. Fr.* **2014**, *85*, 139–149. [CrossRef]
83. Dzingle, J.; Mehta, S.; Chen, P.-J.; Yadav, S. Correction of Unilateral Posterior Crossbite with U-MARPE. *Turk. J. Orthod.* **2020**, *33*, 192–196. [CrossRef]
84. Panamonta, V.; Pradubwong, S.; Panamonta, M.; Chowchuen, B. Global Birth Prevalence of Orofacial Clefts: A Systematic Review. *J. Med. Assoc. Thai.* **2015**, *98* (Suppl. 7), S11–S21.
85. Zhao, C.; Hallac, R.R.; Seaward, J.R. Analysis of Facial Movement in Repaired Unilateral Cleft Lip Using Three-Dimensional Motion Capture. *J. Craniofac. Surg.* **2021**, *32*, 2074–2077. [CrossRef]
86. Kaplan, M.; Gorgulu, S.; Cesur, E.; Arslan, C.; Altug, A.T. 3D evaluation of tooth crown size ın unilateral cleft lip and palate patients. *Niger. J. Clin. Pract.* **2020**, *23*, 596–602. [CrossRef]
87. Huda, N.U.; Shahzad, H.B.; Noor, M.; Ishaq, Y.; Anwar, M.A.; Kashif, M. Frequency of Different Dental Irregularities Associated With Cleft Lip and Palate in a Tertiary Care Dental Hospital. *Cureus* **2021**, *13*, e14456. [CrossRef]
88. Akcam, M.O.; Aydemir, H.; Özer, L.; Özel, B.; Toygar-Memikoğlu, T.U. Three-dimensional tooth crown size symmetry in cleft lip and cleft palate. *Angle Orthod.* **2014**, *84*, 623–627. [CrossRef] [PubMed]
89. Antonarakis, G.S.; Tsiouli, K.; Christou, P. Mesiodistal tooth size in non-syndromic unilateral cleft lip and palate patients: A meta-analysis. *Clin. Oral Investig.* **2013**, *17*, 365–377. [CrossRef] [PubMed]
90. Thierens, L.A.M.; Kerckhof, E.; de Roo, N.M.C.; Temmerman, L.; Nadjmi, N.; Swennen, G.; Ortega-Castrillon, A.; Claes, P.; de Pauw, G.A.M. The Effect of Autologous Alveolar Bone Grafting on Nasolabial Asymmetry in Unilateral Cleft Lip and Palate. *J. Craniofac. Surg.* **2020**, *31*, 1687–1691. [CrossRef] [PubMed]
91. Ben Bouhjar, N.; Kleinheinz, J.; Dirksen, D.; Berssenbrügge, P.; Runte, C.; Wermker, K. Facial and midfacial symmetry in cleft patients: Comparison to non-cleft children and influence of the primary treatment concept. *J. Craniomaxillofac. Surg.* **2019**, *47*, 741–749. [CrossRef] [PubMed]
92. Lewyllie, A.; Cadenas De Llano-Pérula, M.; Verdonck, A.; Willems, G. Three-dimensional imaging of soft and hard facial tissues in patients with craniofacial syndromes: A systematic review of methodological quality. *Dentomaxillofacial Radiol.* **2018**, *47*, 20170154. [CrossRef]
93. Armand, T.; Schaefer, E.; Di Rocco, F.; Edery, P.; Collet, C.; Rossi, M. Genetic bases of craniosynostoses: An update. *Neurochirurgie* **2019**, *65*, 196–201. [CrossRef] [PubMed]
94. Cohen, M.M. Perspectives on craniofacial asymmetry. *Int. J. Oral Maxillofac. Surg.* **1995**, *24*, 191–194. [CrossRef]
95. Meyer, U. Classification of Craniofacial Malformations. In *Fundamentals of Craniofacial Malformations*; Meyer, U., Ed.; Springer: Cham, Switzerland, 2021; pp. 67–84.

96. Kilcoyne, S.; Luscombe, C.; Scully, P.; Jayamohan, J.; Magdum, S.; Wall, S.; Johnson, D.; Wilkie, A.O.M. Language Development, Hearing Loss, and Intracranial Hypertension in Children With TWIST1-Confirmed Saethre-Chotzen Syndrome. *J. Craniofac. Surg.* **2019**, *30*, 1506–1511. [CrossRef]
97. Twigg, S.R.F.; Wilkie, A.O.M. A Genetic-Pathophysiological Framework for Craniosynostosis. *Am. J. Hum. Genet.* **2015**, *97*, 359–377. [CrossRef] [PubMed]
98. Ridgway, E.B.; Ropper, A.E.; Mulliken, J.B.; Padwa, B.L.; Goumnerova, L.C. Meningoencephalocele: A late complication of Le Fort III midfacial advancement in a patient with Crouzon syndrome. *J. Neurosurg. Pediatr.* **2010**, *6*, 368–371. [CrossRef] [PubMed]
99. Xie, C.; De, S.; Selby, A. Management of the Airway in Apert Syndrome. *J. Craniofac. Surg.* **2016**, *27*, 137–141. [CrossRef] [PubMed]
100. Meyer, T. Psychosocial Adjustment of Patients with Congenital Craniofacial Malformations. In *Fundamentals of Craniofacial Malformations*; Meyer, U., Ed.; Springer International Publishing: Cham, Switzerland, 2021; pp. 239–247. ISBN 978-3-030-46023-5.
101. Wong, G.B.; Kakulis, E.G.; Mulliken, J.B. Analysis of fronto-orbital advancement for Apert, Crouzon, Pfeiffer, and Saethre-Chotzen syndromes. *Plast. Reconstr. Surg.* **2000**, *105*, 2314–2323. [CrossRef]
102. Bouaoud, J.; Hennocq, Q.; Paternoster, G.; James, S.; Arnaud, E.; Khonsari, R.H. Excessive ossification of the bandeau in Crouzon and Apert syndromes. *J. Craniomaxillofac. Surg.* **2020**, *48*, 376–382. [CrossRef]
103. Hurmerinta, K.; Kiukkonen, A.; Hukki, J.; Saarikko, A.; Leikola, J. Lambdoid Synostosis Versus Positional Posterior Plagiocephaly, a Comparison of Skull Base and Shape of Calvarium Using Computed Tomography Imaging. *J. Craniofac. Surg.* **2015**, *26*, 1917–1922. [CrossRef]
104. Losee, J.E.; Mason, A.C. Deformational plagiocephaly: Diagnosis, prevention, and treatment. *Clin. Plast. Surg.* **2005**, *32*, 53–64. [CrossRef]
105. Ballesta-Martínez, M.J.; López-González, V.; Dulcet, L.A.; Rodríguez-Santiago, B.; Garcia-Miñaúr, S.; Guillen-Navarro, E. Autosomal dominant oculoauriculovertebral spectrum and 14q23.1 microduplication. *Am. J. Med. Genet. A* **2013**, *161*, 2030–2035. [CrossRef]
106. Seow, W.K.; Urban, S.; Vafaie, N.; Shusterman, S. Morphometric analysis of the primary and permanent dentitions in hemifacial microsomia: A controlled study. *J. Dent. Res.* **1998**, *77*, 27–38. [CrossRef] [PubMed]
107. Perrotta, S.; Bocchino, T.; D'Antò, V.; Michelotti, A.; Valletta, R. Pseudo Hemifacial Microsomia With Condylar-Coronoid Collapse: New Therapeutic Approach in Growing Patients. *J. Craniofac. Surg.* **2020**, *31*, 2128–2131. [CrossRef] [PubMed]
108. Meazzini, M.C.; Brusati, R.; Caprioglio, A.; Diner, P.; Garattini, G.; Giannì, E.; Lalatta, F.; Poggio, C.; Sesenna, E.; Silvestri, A.; et al. True hemifacial microsomia and hemimandibular hypoplasia with condylar-coronoid collapse: Diagnostic and prognostic differences. *Am. J. Orthod. Dentofac. Orthop.* **2011**, *139*, e435–e447. [CrossRef] [PubMed]
109. Sandhu, S.; Kaur, T. Hemifacial microsomia. A case report and review. *Indian J. Dent. Res.* **2002**, *13*, 82–86.
110. Hodzic, Z.; Törnwall, J.; Leikola, J.; Heliövaara, A.; Suojanen, J. Alloplastic Temporomandibular Joint Reconstruction in Congenital Craniofacial Deformities. *J. Craniofac. Surg.* **2021**, *32*, e548–e551. [CrossRef]
111. Podmelle, F.; Metelmann, H.R.; Waite, P. Endoscopic abdominoplasty providing a perforator fat flap for treatment of hemi-facial microsomia. *J. Craniomaxillofac. Surg.* **2012**, *40*, 665–667. [CrossRef]
112. Cassi, D.; Magnifico, M.; Gandolfinini, M.; Kasa, I.; Mauro, G.; Di Blasio, A. Early Orthopaedic Treatment of Hemifacial Microsomia. *Case Rep. Dent.* **2017**, *2017*, 7318715. [CrossRef]
113. Sanjana, M.; Manikandan, S.; Maheshwari, U.; Parameswaran, R.; Vijayalakshmi, D. An Interdisciplinary Management of Severe Facial Asymmetry Due to Hemifacial Microsomia. *Contemp. Clin. Dent.* **2020**, *11*, 387–394. [CrossRef]
114. Qiu, X.; Sun, H.; Zhu, M.; Chen, X.; Chai, G.; Yang, X.; Zhang, Y. Using orthodontic elastic traction during the active period of distraction osteogenesis to increase the effective vertical extension of hemifacial microsomia patients: A multi-center randomized clinical trial. *J. Craniomaxillofac. Surg.* **2021**. [CrossRef] [PubMed]
115. Ainuz, B.Y.; Wolfe, E.M.; Wolfe, S.A. Surgical Management of Facial Port-Wine Stain in Sturge Weber Syndrome. *Cureus* **2021**, *13*, e12637. [CrossRef]
116. Farley, E.; Ariti, C.; Amirtharajah, M.; Kamu, C.; Oluyide, B.; Shoaib, M.; Isah, S.; Adetunji, A.S.; Saleh, F.; Ihekweazu, C.; et al. Noma, a neglected disease: A viewpoint article. *PLoS Negl. Trop. Dis.* **2021**, *15*, e0009437. [CrossRef] [PubMed]
117. Farley, E.; Lenglet, A.; Ariti, C.; Jiya, N.M.; Adetunji, A.S.; van der Kam, S.; Bil, K. Risk factors for diagnosed noma in northwest Nigeria: A case-control study, 2017. *PLoS Negl. Trop. Dis.* **2018**, *12*, e0006631. [CrossRef]
118. Srour, M.L.; Marck, K.; Baratti-Mayer, D. Noma: Overview of a Neglected Disease and Human Rights Violation. *Am. J. Trop. Med. Hyg.* **2017**, *96*, 268–274. [CrossRef] [PubMed]
119. Mahajan, V.K.; Sharma, N.L.; Sharma, R.C. "Were-Wolf" Cutaneous Tuberculosis†. *Int. J. Lepr. Other Mycobact. Dis.* **2004**, *72*, 473. [CrossRef]
120. Eolchiyan, S.A. Complex skull defects reconstruction with CAD/CAMtitanium and polyetheretherketone (PEEK) implants. *Zh. Vopr. Neirokhir. Im. NN Burd.* **2014**, *78*, 3–13.
121. Gerbino, G.; Bianchi, F.A.; Zavattero, E.; Tartara, F.; Garbossa, D.; Ducati, A. Single-step resection and reconstruction using patient-specific implants in the treatment of benign cranio-orbital tumors. *J. Oral Maxillofac. Surg.* **2013**, *71*, 1969–1982. [CrossRef] [PubMed]
122. Gerbino, G.; Zavattero, E.; Zenga, F.; Bianchi, F.A.; Garzino-Demo, P.; Berrone, S. Primary and secondary reconstruction of complex craniofacial defects using polyetheretherketone custom-made implants. *J. Craniomaxillofac. Surg.* **2015**, *43*, 1356–1363. [CrossRef]

123. Zhou, L.; Shang, H.; He, L.; Bo, B.; Liu, G.; Liu, Y.; Zhao, J. Accurate reconstruction of discontinuous mandible using a reverse engineering/computer-aided design/rapid prototyping technique: A preliminary clinical study. *J. Oral Maxillofac. Surg.* **2010**, *68*, 2115–2121. [CrossRef]
124. Villanueva-Alcojol, L.; Monje, F.; González-García, R. Hyperplasia of the mandibular condyle: Clinical, histopathologic, and treatment considerations in a series of 36 patients. *J. Oral Maxillofac. Surg.* **2011**, *69*, 447–455. [CrossRef]
125. Gateno, J.; Coppelson, K.B.; Kuang, T.; Poliak, C.D.; Xia, J.J. A Better Understanding of Unilateral Condylar Hyperplasia of the Mandible. *J. Oral Maxillofac. Surg.* **2021**, *79*, 1122–1132. [CrossRef] [PubMed]
126. Arora, K.S.; Bansal, R.; Mohapatra, S.; Pareek, S. Review and Classification Update: Unilateral condylar hyperplasia. *BMJ Case Rep.* **2019**, *12*, e227569. [CrossRef] [PubMed]
127. Davis, B.K. The role of technology in facial prosthetics. *Curr. Opin. Otolaryngol. Head Neck Surg.* **2010**, *18*, 332–340. [CrossRef]
128. Runte, C.; Dirksen, D.; Deleré, H.; Thomas, C.; Runte, B.; Meyer, U.; von Bally, G.; Bollmann, F. Optical data acquisition for computer-assisted design of facial prostheses. *Int. J. Prosthodont.* **2002**, *15*, 129–132. [PubMed]
129. Feng, Z.; Dong, Y.; Zhao, Y.; Bai, S.; Zhou, B.; Bi, Y.; Wu, G. Computer-assisted technique for the design and manufacture of realistic facial prostheses. *Br. J. Oral Maxillofac. Surg.* **2010**, *48*, 105–109. [CrossRef]
130. Bockey, S.; Berssenbrügge, P.; Dirksen, D.; Wermker, K.; Klein, M.; Runte, C. Computer-aided design of facial prostheses by means of 3D-data acquisition and following symmetry analysis. *J. Craniomaxillofac. Surg.* **2018**, *46*, 1320–1328. [CrossRef]
131. Bechtold, T.E.; Göz, T.G.; Schaupp, E.; Koos, B.; Godt, A.; Reinert, S.; Berneburg, M. Integration of a maxillary model into facial surface stereophotogrammetry. *J. Orofac. Orthop.* **2012**, *73*, 126–137. [CrossRef]
132. Schweiger, J.; Güth, J.-F.; Edelhoff, D.; Stumbaum, J. Virtual evaluation for CAD-CAM-fabricated complete dentures. *J. Prosthet. Dent.* **2017**, *117*, 28–33. [CrossRef]
133. Nellis, J.C.; Ishii, M.; Byrne, P.J.; Boahene, K.D.O.; Dey, J.K.; Ishii, L.E. Association Among Facial Paralysis, Depression, and Quality of Life in Facial Plastic Surgery Patients. *JAMA Facial Plast. Surg.* **2017**, *19*, 190–196. [CrossRef] [PubMed]
134. Sánchez-Ocando, M.; Gavilán, J.; Penarrocha, J.; González-Otero, T.; Moraleda, S.; Roda, J.M.; Lassaletta, L. Facial nerve repair: The impact of technical variations on the final outcome. *Eur. Arch. Otorhinolaryngol.* **2019**, *276*, 3301–3308. [CrossRef]
135. Hontanilla, B.; Olivas-Menayo, J.; Marré, D.; Cabello, Á.; Aubá, C. Maximizing the Smile Symmetry in Facial Paralysis Reconstruction: An Algorithm Based on Twenty Years' Experience. *Facial Plast. Surg.* **2021**, *37*, 360–369. [CrossRef] [PubMed]
136. Fagien, S. Temporary management of upper lid ptosis, lid malposition, and eyelid fissure asymmetry with botulinum toxin type A. *Plast. Reconstr. Surg.* **2004**, *114*, 1892–1902. [CrossRef] [PubMed]
137. de Sanctis Pecora, C.; Shitara, D. Botulinum Toxin Type A to Improve Facial Symmetry in Facial Palsy: A Practical Guideline and Clinical Experience. *Toxins* **2021**, *13*, 159. [CrossRef] [PubMed]
138. Wollina, U.; Goldman, A. Botulinumtoxin-A und dermale Gewebefiller in der fazialen Rehabilitation. *Wien. Med. Wochenschr.* **2017**, *167*, 92–95. [CrossRef]
139. Somani, P.; Nayak, A.K. Restoration of blinking reflex and facial symmetry in a Bell's palsy patient. *Indian J. Dent. Res.* **2011**, *22*, 857–859. [CrossRef] [PubMed]
140. Pathak, C.; Pawah, S.; Sikri, A.; Rexwal, P.; Aggarwal, P. Lip and Lower Lid Supporting Prosthetic Appliance: A Unique Approach of Treating Unilateral Facial Paralysis. *J. Clin. Diagn. Res.* **2017**, *11*, ZD09–ZD11. [CrossRef] [PubMed]